

**Original Paper** ~~~~~

# Effects of Processing Conditions on Tearing Characteristics of Zipper Lines of E-Flute Corrugated Paperboard (Dependency of Length of Connecting Portions, Width of Zipper Band, Phase Shift of Dashed Lines and Tearing Velocity on Tearing Characteristics)

Shigeru NAGASAWA\*†, Kouhei ISHII\* and Itaru KOBAYASHI\*

A structure of zipper band is used for opening a cover or splitting a panel by tearing the zipper dashed lines, which are processed by using a repeatedly nicked (perforation formed) wedge blade. To arrange the geometrical design parameters of the zipper band of a package box, the tearing characteristics of the zipper-connecting portions must be clarified. Herein, to investigate the tearing strength and the success rate of connecting portions (uncut zones) of corrugated board in the fabrication machine direction, the length of connecting portions, the width of zipper band, the phase shift angle between two dashed lines, and the pulling velocity of the cramped end of the zipper band were changed in the tearing test of the zipper band. The experimental results show that the outside (lower side) liner was de-laminated and tore protrusion occurred at the connecting portions in the band area. For the upper critical length of connecting portions, at which the success rate became zero, the upper bound tearing strength was obtained and is related to the Elmendorf-like tearing value by the uniaxial tensile test.

**Keywords:** zipper pull tab, nick, peeling, delamination, grainy, tearing, upper/lower critical length, Elmendorf tearing strength

## 1. Introduction

To easily open a closed packaging box, a method for tearing the zipper band (zipper pull tab) is implemented on the flap of the packaging box. A zipper band for opening a flap of box normally consists of two parallel dashed lines, which are perforations for tearing. There are empirically various cutting patterns of zipper band for each manufacturer. However, there are no public designing methods and theoretical investigations on the mechanics of the tearing characteristics of zipper bands. Regarding the failure behavior of paper, the mode III tear test (out-of-plane shearing) as the Elmendorf test<sup>1,2)</sup>, in which the tear propagates across the sheet parallel to the direction of the initial slit, is known and standardized (e.g., TAPPI, T414). Since this test method evaluates the tear strength of a plain thin paper or paperboard, a certain finite length of the uncut zone should be

analyzed to determine its fracture behavior. In a study by Yamauchi et al.<sup>3)</sup>, the Elmendorf tear index was statistically equal to the tear index of tensile testing of thin papers. Namely, an out-of-plane tearing of paper using the tensile testing method shows a similar tearing resistance as that of the Elmendorf testing. Nagasawa et al. investigated the tearing tensile force and breaking modes of the connecting portions (uncut zones) of a 310g/m<sup>2</sup> white-coated recycled paperboard, while varying some parameters, such as the pitch of the nicks and the profile of entry guide parts<sup>4)</sup>. Consequently, it was reported that appropriate guiding routes embedded in the band zone contributed to the truncation of connecting portions when the band's perforation was across the grain direction. The upper or lower critical length of connecting portions, at which the tearing success rate of connecting portions

\* Nagaoka University of Technology, Dept. of Mechanical Eng.,

† Corresponding author, ditto. 1603-1 Kamitomioka, Nagaoka, Niigata 940-2188, Japan,  
TEL/FAX: +81-258-47-9701, Email: snaga@mech.nagaokaut.ac.jp

became zero or started to decrease, was reported, and the effects of the inclined pulling direction on the tearing success rate was investigated for a 310g/m<sup>2</sup> paperboard<sup>5,6</sup>). Josip Bota et al. compared different zipper tear strips (ZTS) and conducted a manual opening test<sup>7</sup>). However, these reports were limited to a certain paperboard thickness ( $t=0.3\text{--}0.4\text{mm}$ ). Besides, studies on the tearing behavior of corrugated boards have not been conducted.

Herein, to reveal the effects of the processing conditions (the length and width of connecting portions, the inclined pulling direction, the phase shift and the tearing velocity) on the breaking modes and the tearing success rate of connecting portions (uncut zones) of an E-flute corrugated board, a tearing test of zipper lines was experimentally investigated when dashed-cutting lines were across the flutes as  $\phi=0^\circ$  (parallel to the fabricating machine direction of the corrugated board).

## 2. Experimental

### 2.1 Specimens

Fig.1 shows a schematic illustration of the double-faced corrugated board, which is composed of the upper (front side) liner, lower (backside) liner and the corrugated medium (CM). The nominal specifications of E-flute board prepared are as follows: board height  $t=1.5\text{mm}$ , wave numbers of the CM  $93\pm5$  for 300mm (wavelength 3.4–3.1mm), Liners' basis weight 160g/m<sup>2</sup>, C5 liners' thickness 0.220mm, CM basis weight 115g/m<sup>2</sup> and CM thickness 0.166mm (JIS P 8118).

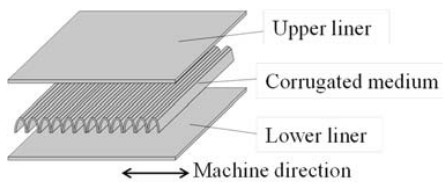
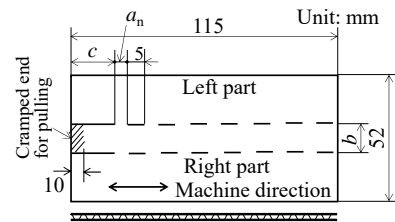


Fig.1 Schematic illustration of corrugated paperboard

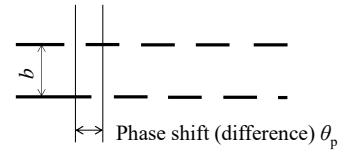
Fig.2 shows the basic layout and size of the specimen for the zipper band tearing test. The parameters of the geometrical pattern of the

zipper are as follows: length of dashed-cutting line = 5mm, connecting portions' length (uncut zones)  $a_n=2, 2.5, \text{ and } 3\text{mm}$ , zipper band width  $b=12, 15, 20, \text{ and } 25\text{mm}$ , and phase shift angle  $\theta_p=0^\circ, 90^\circ, \text{ and } 180^\circ$ .

Herein, the band strip is composed of two dashed lines of  $a_n+5\text{mm}$  (cutting line) with the phase shift angle  $\theta_p$ , as shown in Fig.2 (b). The difference between the left part and right part was calculated as  $(\theta_p/360)(a_n+5)$ .



(a) Layout and size of specimen for tearing test



(b) Phase shift (difference) of two perforations

Fig.2 Specimen for tearing test.

The two dashed-cutting lines were processed using a high-carbon-steel blade (NSK, KG 42417444), which had an angular aperture and crossing angle of  $20.5^\circ$  and  $18.4^\circ$ , respectively. Since the cutting process was two-way as shown in Fig.3, the end profile of the cutting lines was made in the right-angle shape. After processing two-way cutting, the upper length of cutting  $L$  and the lower length of cutting  $l$  became equal with each other. For the clamped end of the band for pulling up, the length of the first cutting line  $c=15\text{mm}$  was prepared, and the 10mm hatched was initially hand-bent at a right angle. All experiments were classified into two groups as follows. (i) When the phase shift affected the tearing characteristics,  $b$  was fixed at 12mm, whereas  $a_n$  was chosen as 2–3mm. Table 1 arranges all patterns. (ii) When  $b$  affected the tearing

characteristics,  $\theta_p$  was set as  $0^\circ$ , whereas  $a_n$  was set as 2–3mm. Table 2 arranges all patterns.

Specimens were prepared in a room at an average temperature of 296K and relative humidity of 50% for 48h. The Number of specimens was five for each zipper pattern.

## 2.2 Experimental method

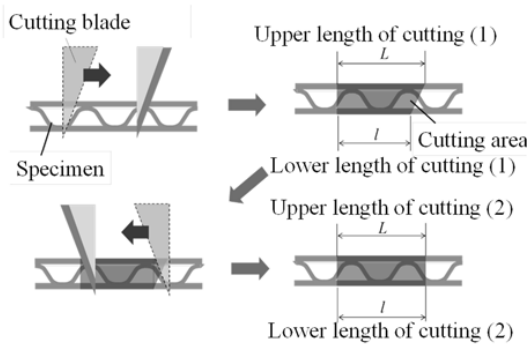
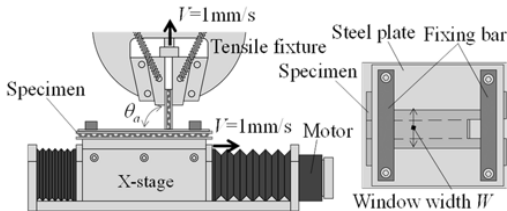


Fig.3 Two-way cutting of specimen



(a) Pulling claw and X-stage (b) Fastening  
Fig.4 Schematics of experimental apparatus.

Fig.4 shows the experimental apparatus for the tearing test of a corrugated board. The apparatus is composed of a uniaxial tensile testing apparatus with tearing velocity  $V$  and an X-stage with horizontal moving velocity  $V$ . The usual velocity was set as  $V=1\text{mm/s}$ . In contrast, it was set as 0.5, 1 and 5mm/s for investigating the velocity effect on tearing. Here, the angle of the pulling direction  $\theta_a$  of the zipper band's clamped end was set as  $90^\circ$  against the horizontal X-stage. Due to the restriction of the moving device, the total displacement of the zipper band's clamped end was 40mm.

Table 1 Patterns of zipper lines in group (i), band width  $b=12\text{mm}$ .

Type of pattern	A	B	C	D	E	F	G	H	I
Length of uncut zone $a_n/\text{mm}$	2			2.5			3		
Angle of phase shift $\theta_p/^\circ$	0	90	180	0	90	180	0	90	180

Table 2 Patterns of zipper lines in group (ii), phase shift angle  $\theta_p=0^\circ$ .

Type of pattern	a	b	c	d	e	f	g	h	i
Length of uncut zone $a_n/\text{mm}$	2			2.5			3		
Width of band $b/\text{mm}$	15	20	25	15	20	25	15	20	25

Consequently, five uncut zones (five stages) were torn on the dashed lines of the E-flute specimen. When the specimen was fastened using a window-opened steel plate at  $b=12$  and 15mm, the window's width  $W$  was set as 20mm, whereas for  $b=20$  and 25mm,  $W$  was set as 50mm, respectively.

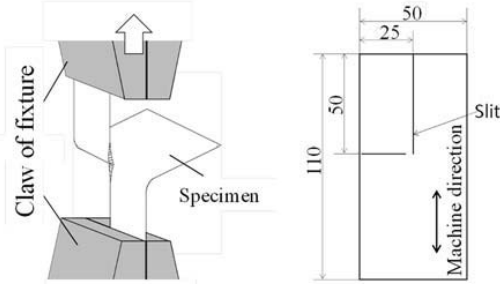
In the tearing test, the relationship between the tearing tensile force  $F$  and the displacement of the clamped end of the zipper band  $x$  was measured for five stages of connecting portions. The maximum peak tearing forces  $F_{pi}$  ( $i=1,2,3,4$  and 5) were detected from the response. During the process, a digital camera recorded the tearing behavior of the specimen, and the success rate of separation of five connecting portions  $p_s$  and the failure rate of separation at any stage ( $i=1-5$ )  $p_{Fi}$  was investigated. Here,  $p_s + \sum_{i=1}^5 p_{Fi} = 1$ . When investigating the dependency of the tearing characteristics on the tearing velocity,  $b$  was set as 12mm and five specimens were used for each velocity.

## 2.3 Fundamental tearing strength

To evaluate the fundamental tearing strength of the E-flute corrugated board in the machine direction (across flute), an Elmendorf-like tearing strength test was conducted using a uniaxial tensile device (Fig.5).

with parameters:  $c=20\text{mm}$ ,  $b=12\text{mm}$ , and  $a_n=90\text{mm}$  (Fig.2(a)), was prepared and was tested (tearing test) under  $V=1.67\text{mm/s}$ . Five

specimen were used for the test. This method used a sufficiently long connecting portion to estimate the upper bound tearing strength of the zipper band<sup>5)</sup>.



(a) Tensile for tearing (b) Specimen (Unit:mm)  
Fig.5 Schematics of tearing test by uniaxial tensile.

## 2.4 Fundamental strength of bending moment

A certain maximum peak-bending moment is experimentally observed when considering a cantilever bending of a band strip in the machine direction. With a 10mm loading position length from the clamped end of a bending strength tester CST-J-1<sup>8)</sup>, the bending moment resistance of the E-flute corrugated board was measured with respect to the folding angle. Using this bending moment response, the maximum peak-bending moment was investigated, knowing the fundamental bending strength at the first stage.

## 3. Results and discussion

### 3.1 Fundamental tearing strength

Fig.6 shows examples of the line-bending moment resistance  $M$  of the non-creased E-flute board for the folding angle  $\theta=0^\circ-90^\circ$  when the bending line was parallel to the flute direction. For  $\theta>10^\circ$ , since the folded-inside liner was buckled at a valley position of the intermediate wave layer,  $M$  was smaller than the maximum peak  $M_{\text{peak}}$  (2.9 N in average) at  $\theta_{\text{peak}}$  ( $5.2^\circ$  in an average of five samples).  $M_{\text{peak}}$  is related to the bending resistance of the specimen at the first stage of the pull-up motion.

Fig.7 shows an example of the tearing force response using the apparatus and specimen shown in Fig.5.

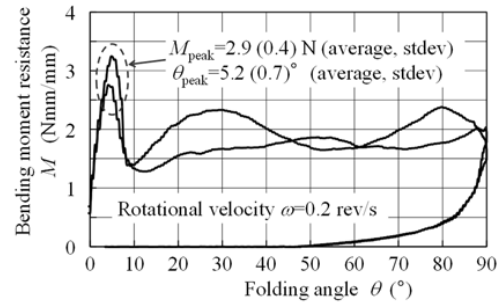


Fig.6 Bending moment resistance of non-creased E-flute board in parallel to flute.

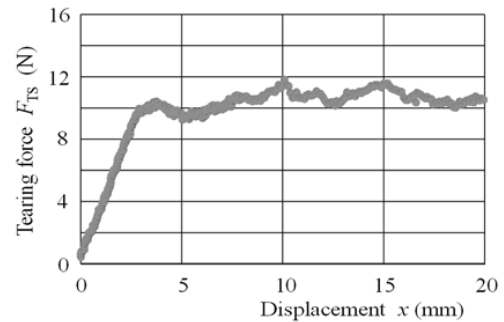


Fig.7 Elmendorf-like tearing force using the uniaxial tensile shown in Fig.5, with pulling velocity of 1.67mm/s.

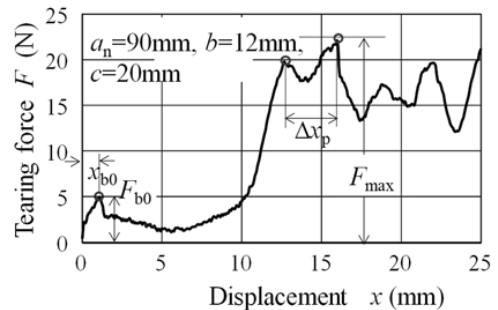


Fig.8 Tearing force response of zipper band when choosing a long uncut zone of 90mm, with pulling velocity of 1.67 mm/s, and  $\theta_a = 90^\circ$ .

The tearing force  $F_{TS}$  almost saturated as 9–12 N for the clamped end's displacement  $x=5-20$ mm. The maximum force at  $x=5-20$ mm was collected to evaluate the Elmendorf-like tearing strength from the test. The average maximum tearing strength for five samples was determined as 11.41N, with a standard deviation of 1.25N.

Fig.8 shows an example of the tearing force  $F$  in Fig.4 when choosing a long connecting portion ( $a_n = 90\text{mm}$ ). Half of the maximum tearing force  $F_{\max}/2$  was determined as the average of  $10.85\text{N}$  and with a standard deviation of  $0.95\text{N}$ . Here,  $F$  gradually decreased at  $x > 30\text{mm}$  due to the tearing failure. To a certain extent, in the tearing process, a periodic change of  $F$  was observed as peak-to-peak  $\Delta x_p \approx \lambda$  (as wave-length) (Fig.8). Fig.7 and Fig.8 show that  $F_{\max}/2$  was almost equal to an Elmendorf-like tearing strength  $F_{TS}$ . Hence, the tearing strength of the E-flute corrugated board in the machine direction was evaluated as  $F_{TS} = 11\text{N}$  with respect to the tearing line. As the early maximum peak, a position of  $x_{b0} = 1.5\text{mm}$ ,  $F_{b0} = 4.8\text{N}$  was detected (Fig.8). Since the arm length of the pulling point was a projection of the bent-up band  $a_{b0} = \sqrt{((c-10)^2 - x_{b0}^2)} \approx 9.9\text{mm}$ , with  $b=12\text{mm}$ , the bending moment of  $F_{b0}a_{b0}$  was determined as  $4.0\text{Nmm/mm}$ , which appears to be equivalent to  $M_{\text{peak}}$  (Fig.6).

As a referenced investigation, the Elmendorf tearing test using the uniaxial tensile device was applied to a liner sheet of  $160\text{g/m}^2$  ( $0.220\text{mm}$  thick), while varying the tearing velocity  $V$  from  $0.5$  to  $5\text{mm/s}$ . The tearing strength in MD was  $2.0\text{--}2.1\text{N}$ , which gradually increased with  $V$ . The strength of the prepared E-flute corrugated board was about five times stronger than that of the liner sheet. Here, the tearing strength of the liner sheet in CD was  $1.5\text{--}2.0\text{N}$  for  $V = 0.5\text{--}5\text{mm/s}$ . The results indicated that the tearing strength of the raw liner sheet increased as the tearing velocity increased.

### 3.2 Effect of length of connecting portions on tearing

Fig.9 shows the side views of the pull-up zipper band, with  $b = 12\text{mm}$ ,  $a_n = 2\text{mm}$ , and  $\theta_p = 0^\circ$  (type A). Fig.10 shows the top views of torn connecting portions when choosing types A, D, and G:  $a_n = 2, 2.5$  and  $3.0\text{mm}$  at  $\theta_p = 0^\circ$ ,  $b = 12\text{mm}$ . Fig.11 shows the failure mode occurring at the third stage during the tearing test in type D ( $a_n$

$= 2.5\text{mm}$ ,  $\theta_p = 0^\circ$ ). The success rate of the tearing separation  $p_s$  was  $100\%$ ,  $80\%$  and  $0\%$  for types A, D and G, respectively.

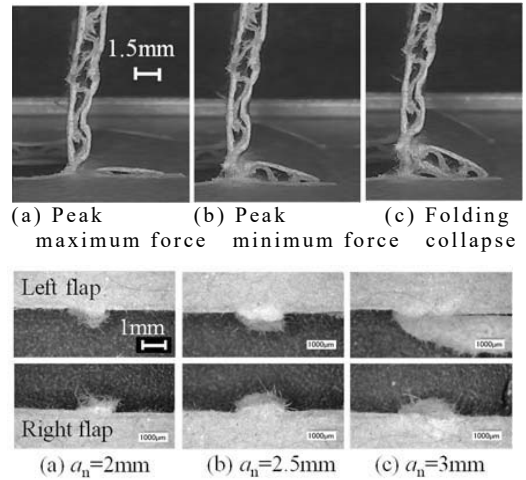


Fig.10 Top views of front side, torn connecting portions for types A, D, G.

Namely, the upper critical length, at which  $p_s = 0$ , was  $a_n = 3\text{mm}$  ( $a_n/t=2$ ), and the lower critical length, at which  $p_s$  started decreasing, was  $a_n = 2\text{mm}$  ( $a_n/t=1.33$ ) for types A, D and G.

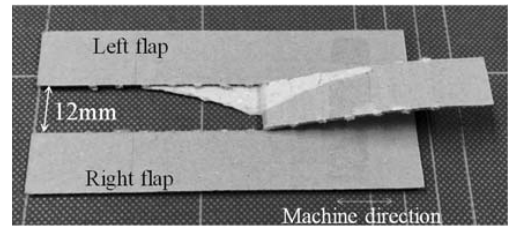


Fig.11 General view of failure mode of tearing at type D.

Torn protrusion occurred at the band and the left/right-side area, although the band strip seemed a little plucked. Fig.10(c) and Fig.11 show that the tearing failure mode started from the lower liner, outside the folded band strip. This pull-out tendency of the band strip was like that of a white-coated paperboard<sup>5,6)</sup>.

Fig.12 shows representative examples of the tearing tensile force  $F$  with respect to the displacement  $x$  with  $a_n = 2, 2.5$  and  $3\text{mm}$  at  $b = 12\text{mm}$ ,  $\theta_p = 0^\circ$  (A, D and G). At the early first stage ( $x=2\text{--}5\text{mm}$ ) in Fig.12, the peak minimum force was detected. The similar peak minimum forces were also detected in the second, third,

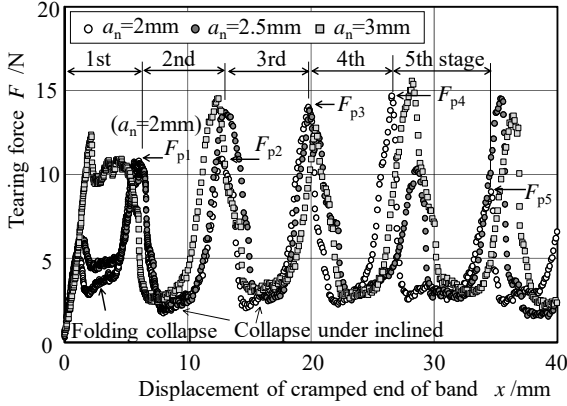


Fig.12 Representative relationship between tearing force and displacement of cramped end of band strip for types A, D, G.

fourth and fifth stages. The resistance can be attributed to the plastic collapse<sup>9)</sup> of the folded band strip. After the folding collapse at each stage, the tearing force reached  $F_{pi}$  ( $i=1,2,3,4$ , and 5). Although plastic collapse principally occurred at every stage (connecting portion), the first stage collapse was relatively larger than that after the second stage due to a certain inclined attitude of the pull-up band. Here, the folded position and its resistance dispersed among the specimens due to the periodic rigidity of CM. The maximum peak forces also disperse, as seen in Fig.12. Table 3 shows the average maximum peak force  $F_p$  and its standard deviation for the five stages. The full-average force  $F_p$  of five stages  $F_{pi}$  ( $i=1-5$ ) was derived as approximation Eq.(1). Here,  $F_p = (\sum_{i=1}^5 F_{pi})/5$  and  $F_{TS} = 11\text{N}$  as described in section 3.1. The tearing force increased with the length of connecting portions.

Table 3 Average tearing force  $F_p$  (A,D,G).

$a_n$ /mm	2	2.5	3
$\theta_p$ /°	0		
$F_p$ /N	12.1	12.6	13.5
Std.dev. /N	1.1	1.6	1.4

$$F_p = 11.08 (a_n/t)^{0.28}$$

$$F_p = 0.50(2F_{TS})(a_n/t)^{0.28} \quad (1)$$

### 3.3 Phase shift effect on tearing off

Fig.13 shows the success rate of the tearing separation of connecting portions for all types A-I in group (i). For  $a_n=2.5\text{mm}$ , it was found that the phase shift of the cutting lines slightly reduced the success rate.

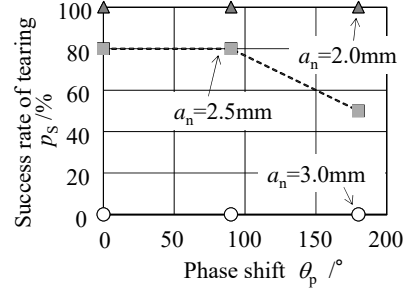


Fig.13 Success rate of tearing of connecting portions for group (i) (types A-I)

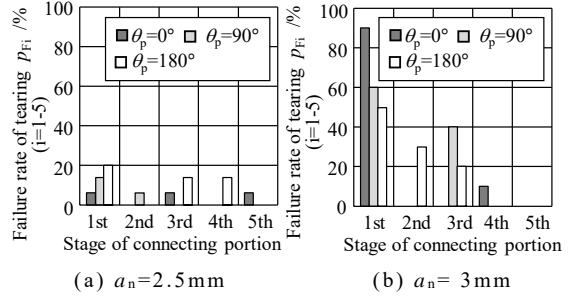


Fig.14 Tearing failure rate for five stages when choosing types D-I.

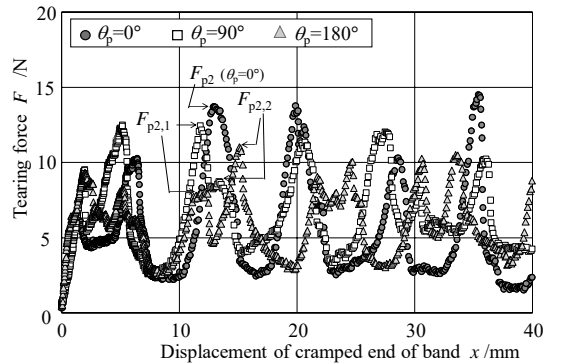


Fig.15 Representative relationship between tearing force and displacement of cramped end of zipper band for types D, E, and F.

Fig.14 shows that the failure rate of tearing scattered in the five stages, whereas Fig.15 shows a representative relationship between the

tearing force and the displacement of the clamped end of the band strip when changing  $\theta_p=0^\circ, 90^\circ$ , and  $180^\circ$ . Comparing the non-zero phase shift  $\theta_p=90, 180^\circ$  with  $\theta_p=0^\circ$ , as seen in Fig.15, the maximum peak  $F_{pi}$  ( $i=2$  was focused in here) at non-zero phase shift was smaller than that of the zero shift ( $\theta_p=0$ ), and it was divided into two peaks which were denoted as  $F_{p2,1}$  (early peak) and  $F_{p2,2}$  (late peak). This phenomenon arises from the non-zero phase shift of the two dashed-cutting lines (Fig.16). Calculating the full average of the five maximum peak forces  $F_p = (\sum_{i=1}^5 F_{pi})/5$ , Table 4 was derived. For  $a_n=2.5$  and  $3\text{mm}$  at  $\theta_p=180^\circ$ , the maximum peak force was reduced about 21% from  $\theta_p=0^\circ$ . If the right-side tearing is isolated from the left side tearing, the expected maximum peak force seems to be half of the force at the synchronous state as  $\theta_p=0^\circ$ . However, the real pulling force was interfered from the opposite side under a twisted mode of the zipper band.

Table 4 Average tearing force for five stages  $F_p$  (for types B,C,E,F,H, and I).

$a_n/\text{mm}$	2		2.5		3	
$\theta_p/^\circ$	90	180	90	180	90	180
$F_p/\text{N}$	10.6	8.9	11.4	10.0	13.3	10.7
Std.dev./N	1.7	0.6	0.8	1.2	1.5	1.1

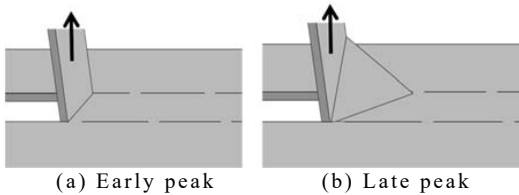


Fig.16 Schematics of twisted-pull band by phase shift of two dashed-cutting lines.

### 3.4 Effect of band width on tearing off

To investigate the effects of band width on the tearing characteristics, the width of the band strip was additionally chosen as  $b=15\text{--}25\text{mm}$  when  $\theta_p$  was maintained as  $0^\circ$  (group ii). Fig.17 shows the success rate of tearing  $p_s$ , whereas Fig.18 shows the failure rate of tearing at any stage  $p_{fi}$  ( $i=1\text{--}5$ ) when changing  $b$ .

In Fig.17, the three cases ( $a_n=2, 2.5$  and  $3.0\text{mm}$ ) at  $b=12\text{mm}$  were rewritten from that of  $\theta_p=0^\circ$  in Fig.13. It was found that the tearing success rate increased with the width of the band strip, and the tearing failure rate was scattered for the five stages.

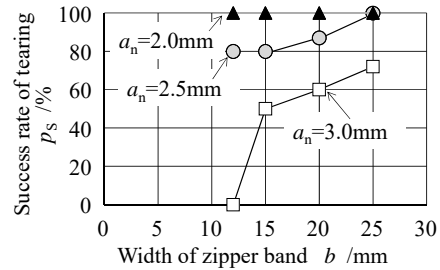


Fig.17 Success rate of tearing for types A, D, G and a-i.

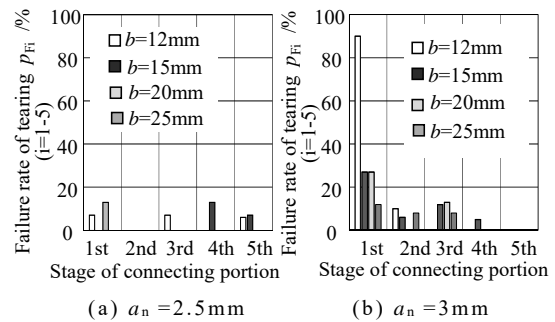


Fig.18 Failure rate of tearing for types a-i.

The success rate increment tendency by the band's width was like that of a white-coated paperboard<sup>6)</sup>. The bending stiffness of the band increases as its width increases. In contrast, the tearing resistance (force) at a connecting portion is determined by the length of the connecting portion. This relation increases the bending curvature radius of the pull-up band when increasing the band's width. This situation was observed, as shown in Fig.19. Fig.19(a) ( $a_n=3\text{mm}$ ) is like Fig.9(a) ( $a_n=2\text{mm}$ ) with respect to the bending angle of the pull-up band. For  $b=25\text{mm}$ , as shown in Fig.19(b), the bending angle of the pull-up band was about  $61^\circ$  at the maximum peak force. Therefore, the in-plane tensile stress of the outside layer of the band strip was reduced, compared to that of  $b=12\text{mm}$ . Thus, the success rate of tearing seems to increase with the width of the band strip.

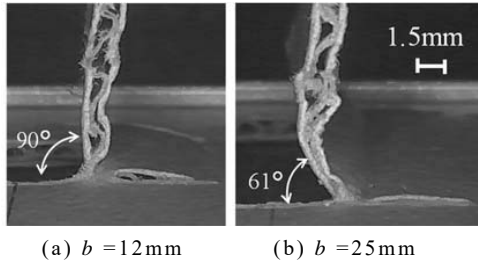


Fig.19 Side views of pull-up band strip at types G and I ( $a_n=3\text{mm}$ ).

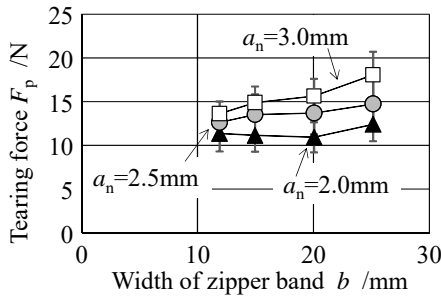


Fig.20 Maximum peak force of tearing for types A, D, G and a-i.

For the tearing force against the width of the band, Fig.20 shows  $F_p$  (as a full average of five stages) for types of A, D, G and a-i. Here, error bars represent the standard deviation of samples.  $F_p$  increased as  $b$  due to the difference in the bending attitude. However, since the upper bound tearing force is expected as  $2F_{TS}=22\text{N}$ ,  $F_p$  seems to settle down into a certain resistance  $< 2F_{TS}$  as  $b$  increases. According to the result of white-coated paperboard<sup>6)</sup>, the tearing force was determined by the length of a connecting portion  $a_n$ , but independent from  $b$ .

### 3.5 Effect of velocity on tearing off

Regarding the tearing velocity effects on the separation of connecting portions, as a plain liner sheet of  $160\text{g/m}^2$  ( $0.220\text{mm}$ ) was explained in section 3.1, the tearing resistance and the deformation of the E-flute specimen seem to be affected by the velocity. Table 5 shows the success rate of tearing for types D and G with the tearing velocities  $V$  of 0.5, 1.0 and 5.0mm/s.

Table 5 Success rate of tearing of connecting portions for types D, G when changing the tearing velocity.

$a_n$ (mm)	2.5	3
$V$ (mm/s)	Success rate $p_s$ (%)	
0.5	80	0
1	80	0
5	90	70

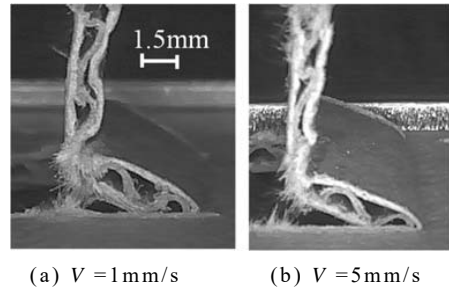


Fig.21 Comparison of side views of pull-up zipper band when changing the tearing velocity at type D.

The tearing state of  $V=0.5\text{mm/s}$  was not sensitive, compared to the case of  $V=1.0\text{mm/s}$ . However, the tearing state of  $V=5\text{mm/s}$  varied, and the success rate increased. Fig.21 shows the side views of the pull-up band when  $V=1.0$  and  $5.0\text{mm/s}$  at  $a_n=2.5\text{mm}$  and  $b=12\text{mm}$ . Comparing Figs. 21 (a) and (b), the torn protrusion of (b) was seen as a small broken volume. Namely, a pull-out deformation at the connecting portion seems to be restricted by the tearing velocity or the strain-rate of that region.

## 4. Conclusions

A plain zipper band without a guiding route was prepared using a 160(upper liner)-115(medium)-160(lower liner)  $\text{g/m}^2$  E-flute corrugated board (total height  $t=1.5\text{mm}$ ). A tearing test of the zipper band was conducted while changing the length of connecting portions  $a_n$ , the width of band strip  $b$ , the angle of the phase shift of the two dashed-cutting lines  $\theta_p$  and the tearing velocity  $V$ . The following conclusions were deduced from the experiments.



- (1) An in-plane tensile test based on fundamental tearing strength was conducted for an E-flute corrugated board and a liner sheet in MD. The E-flute corrugated board, which had a strength of  $F_{TS} = 11\text{N}$ , was about five times stronger than that of the liner sheet.
- (2) The relationship between the full average of the maximum peak tearing force  $F_p$  and the normalized length of the connecting portion  $a_n/t$  was revealed using experimental approximation with an exponentiation rule.
- (3) When choosing the phase shift of two dashed-cutting lines as  $\theta_p = 0^\circ, 90^\circ$ , and  $180^\circ$ ,  $F_p$  decreased and divided into two peaks with  $\theta_p$ . For the tearing state of connecting portions, the success rate decreased slightly at  $\theta_p = 180^\circ$ , but it was unaffected at  $\theta_p = 90^\circ$ .
- (4) When choosing the width of band strip  $b$  as 12, 15, 20, and 25mm, the success rate increased with  $b$  due to the variation of the folding attitude, which was affected by the bending stiffness of the band strip.
- (5) When the tearing velocity was increased from 1 to 5mm/s, the success rate of tearing at connecting portions of the E-flute corrugated board was stably increased.

In many real problems, the tearing velocity seems to be larger than that of this study. When the thickness of corrugated board is larger than that of E-flute, the tearing behavior of zipper seems to be changed. These geometrical and dynamic effects on the tearing characteristics should be investigated furthermore.

## Nomenclature

$b$ : width of the band strip (pull tab),  $b=12, 15, 20$ , and  $25$  (mm)  
 $a_n$ : length of a connecting portion (uncut zone) along the cutting line  
 $\theta_p$ : angle of phase shift (difference) between two dashed-cutting lines,  $\theta_p =$

$0, 90$  and  $180$  ( $^\circ$ )

$F$ : tearing tensile force of the clamped end of the zipper band

$x$ : displacement of the clamped band end in the vertical direction

$F_{pi}$ : the maximum peak tearing force at the  $i$ -th stage (the  $i$ -th connecting portion,  $i=1-5$  was considered)

$F_p$ : average maximum peak tearing force for the five stages,  $(\sum_{i=1}^5 F_{pi})/5$

$ps$ : success rate (probability) of tearing separation of connecting portions by pulling a clamped end of zipper band

$pr_i$ : failure rate of tearing at the  $i$ -th stage.

$F_{TS}$ : (Elmendorf-like) tearing strength using uniaxial tensile test device shown in Fig.5

## 9. References

- 1) C.A.Bronkhorst, K.A.Bennet, Handbook of Physical Testing of Paper, 1, p.388 (1983).
- 2) M.B.Lyne, M.A.Jackson & A.E.Ranger, The in-plane, Elmendorf, and edge tear strength properties of mixed furnish papers, TAPPI, 55(6), p.924 (1972).
- 3) T.Yamauchi, A.Tanaka, Tearing test for paper using a tensile tester, Journal of Wood Science, 48, p.532 (2002).
- 4) S.Nagasawa, M.Uehara & C.Matsumoto, Effects of guiding routes and grain direction of white-clay-coated paper board on tearing characteristics of zipper pull tab (in Japanese), Journal of the Japan Society for Technology of Plasticity, 59(685), p.15 (2018).
- 5) S.Nagasawa, M.Uehara & C.Matsumoto, Tearing characteristics of zipper pull tab of paperboard (in Japanese), Proceedings of 26th annual congress of SPSTJ, p.140 (2017).
- 6) S.Nagasawa, M.Uehara & C.Matsumoto, Effects of mechanical conditions on tearing characteristics of zipper band made of white-clay-coated paperboard (Dependency of tearing characteristics on length of connecting portions, width of band and

- pulling direction), Journal of Advanced Mechanical Design, Systems and Manufacturing, 15(1), p. jamdsm0009 (2021).
- 7) J. Bota, G. Petković, Evaluation of Zipper Tear Strip Design Structure for Paperboard Packaging, Proceedings of International Symposium Graphic Engineering and Design -GRID 2020, At: Novi Sad, Srbija, p.299 (2020).
- 8) Katayama Steel Rule Die Inc., Crease Stress Tester CST-J-1 (online), available from [http://diemex.com/sale/cst\\_e.html](http://diemex.com/sale/cst_e.html), (accessed on 17 February, 2021).
- 9) H.Kudo, Plasticity, Morikita publishing, (1968), pp.16-19 (in Japanese).
- (Received 31 May 2021)  
(Accepted 21 October 2021)